

The Galaxy Luminosity Function from $M_R = -25$ to $M_R = -9$.

Neil Trentham¹, Leda Sampson¹ & Manda Banerji¹

¹ *Institute of Astronomy, Madingley Road, Cambridge, CB3 0HA.*

20 September 2018

ABSTRACT

Redshift surveys like the Sloan Digital Sky Survey (SDSS) have given a very precise measurement of the galaxy luminosity function down to about $M_R = -17$ ($\approx M_B = -16$). Fainter absolute magnitudes cannot be probed because of the flux limit required for spectroscopy. Wide-field surveys of nearby groups using mosaic CCDs on large telescopes are able to reach much fainter absolute magnitudes, about $M_R = -10$. These diffuse, spiral-rich groups are thought to be typical environments for galaxies so their luminosity functions should be the same as the field luminosity function. The luminosity function of the groups at the bright end ($M_R < -17$) is limited by Poisson statistics and is far less precise than that derived from redshift surveys. Here we combine the results of the SDSS and the surveys of nearby groups and supplement the results with studies of Local Group galaxies in order to determine the galaxy luminosity function over the entire range $-25 < M_R < -9$. The average logarithmic slope of the field luminosity function between $M_R = -19$ and $M_R = -9$ is $\alpha = -1.26$, although a single power law is a poor fit to the data over the entire magnitude range. We also determine the luminosity function of galaxy clusters and demonstrate that it is different from the field luminosity function at a high level of significance: there are many more dwarf galaxies in clusters than in the field, due to a rise in the cluster luminosity function of $\alpha \sim -1.6$ between $M_R = -17$ and $M_R = -14$.

Key words: galaxies: luminosity function, mass function

1 INTRODUCTION

The galaxy luminosity function (LF) $\phi(L)$ is defined such that $\phi(L)dL$ is the density of galaxies having luminosities between L and $L + dL$. It is usually regarded as a convenient test of galaxy formation theories because it is so easy to measure. However, the observed galaxy LF is different from the galaxy mass function, which is more directly predicted by theory. This difference is particularly significant in the context of cold dark matter galaxy formation theories (Moore et al. 1999; Klypin et al. 1999; Bullock, Kravstov & Weinberg 2001; Chiu, Gnedin & Ostriker 2001; Benson et al. 2003a,b; Kazantzidis et al. 2004).

There are a number of redshift surveys that have recently been completed. These surveys measure redshifts and therefore distances for large numbers of galaxies in flux-limited samples. The largest such survey is the Sloan Digital Sky Survey (SDSS; www.sdss.org) which has measured redshifts for $> 10^5$ galaxies. The LF produced by this survey has very small uncertainties. The Poisson errors are negligible due to the sample size, and the sample is complete because the vast majority of high-luminosity galaxies have

high surface brightnesses (Cross et al. 2001) and so are contained within the sample. A number of other surveys (see Section 2) also have produced accurate LFs, all of which are consistent with each other given the uncertainties that come from matching the different filters used in the different surveys and from cosmic variance. The SDSS redshift sample is only complete to absolute magnitudes of about $M_R = -17.5$. This limit is imposed by the requirement that galaxies need to be bright enough for spectroscopy. The spectroscopy limit is quite bright because the SDSS uses a relatively small (2.5 m) telescope.

Another recent development has been the advent of mosaic CCDs that can be used on large telescopes (e.g. SuprimeCam on the NAOJ Subaru 8 m Telescope; Miyazaki et al. 2002). This has permitted observations of large areas of sky down to very faint limits. A number of low-surface-brightness galaxies are seen in fields within galaxy groups but not in blank fields. These are interpreted as dwarf galaxies in the group, not background galaxies (Flint et al. 2001a). We can therefore infer their distances without spectroscopy, which is not possible for these faint low-surface-brightness galaxies. Hence measurements of the

LF in nearby (< 20 Mpc) groups are possible down to $M_R = -10$.

Diffuse, spiral-rich groups are typical environments for most galaxies. Therefore it should be possible to append the LFs of these groups to the field LF from SDSS and obtain the galaxy LF over a very wide magnitude range. This is the subject of the present paper.

At the very faint end ($M_R \sim -10$), the surveys of groups run into difficulty because of the inability to assign memberships to faint low-surface-brightness galaxies. At $R > 22$, low-surface-brightness ($\mu > 25$ R mag arcsec $^{-2}$ over 2 or more seeing disks) galaxies appear in blank field surveys. Thus, while excess numbers of low-surface-brightness galaxies may be seen in the group fields, we can only infer group membership in a statistical sense. For example, none of the candidate galaxies with $M_R > -11$ in the diffuse groups studied by Trentham & Tully (2002) can be regarded as highly probable members on an individual basis.

The only environment where the LF can be measured fainter than $M_R = -10$ is the Local Group (the faintest galaxy in the Local Group, Andromeda IX, has $M_R = -9$; Zucker et al. 2004). We therefore supplement the combined SDSS+Groups LF with the Local Group LF at the very faint end.

The paper is structured as follows. In Section 2 we describe results from redshift surveys. In Section 3 we investigate the behaviour of the LF at very bright magnitudes ($M_R < -23$). In Section 4 we describe results from deep wide-field surveys of groups. In Section 5 we compute the R -band Local Group LF. In Section 6 we combine all the individual LFs to determine the galaxy LF between $M_R = -25$ and $M_R = -9$. In Section 7 we investigate analytic forms that describe this function. In Section 8 we do a brief comparison with theory. In Section 9 we compute the cluster LF and investigate how it is different from the field LF. Finally in Section 10 we summarize. Throughout this work, we assume the following cosmological parameters: $H_0 = 65$ kms $^{-1}$ Mpc $^{-1}$, $\Omega_{\text{matter}} = 0.3$, $\Omega_{\Lambda} = 0.7$.

2 RESULTS FROM REDSHIFT SURVEYS

The SDSS LF is most appropriate for this study because its r' filter is similar to the R filter that was used in CCD mosaic studies of nearby groups. It is derived from measurements of $> 10^5$ galaxies so the statistical uncertainties are small. There are a number of other redshift surveys which have similarly produced field LFs (Table 1).

The SDSS LF is described in detail by Blanton et al. (2001, 2003). In Figure 1 we present the SDSS LF converted to the R magnitude system that we use in this paper.

3 THE VERY BRIGHT END

At the very bright end the SDSS LF is not a direct measurement. This is because most of the galaxies in the SDSS sample with $M_R < -23$ are sufficiently distant that evolutionary corrections to redshift zero are significant. Figure 2 shows that at absolute magnitudes $M_R < -23$ the majority of galaxies have redshifts $z > 0.2$, where corrections are typically 0.3 mag (Lin et al. 1999; Blanton et al. 2003).

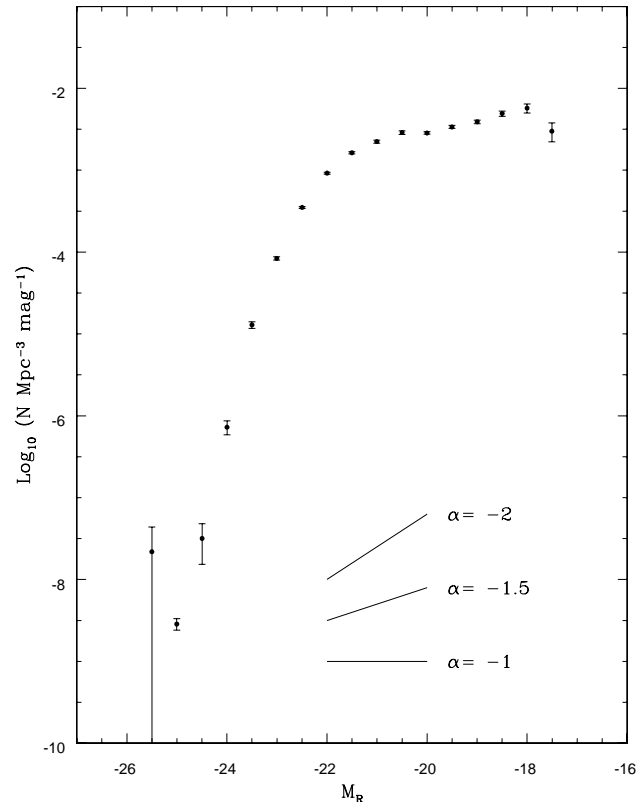


Figure 1. The SDSS luminosity function, from Blanton et al. (2003), corrected to our cosmology. This is derived from the SDSS r' LF assuming a colour correction of $r' - R$ varying from 0.24 at $M_R = -24$ to 0.17 at $M_R = -16$. These conversions come from the calibrations of Fukugita, Shimasaku and Ichikawa (1995) and the colour-dependent LFs of Blanton et al. (2001). Three values of $\alpha = d \log \phi(L) / d \log L$, the logarithmic slope of the luminosity function, are shown.

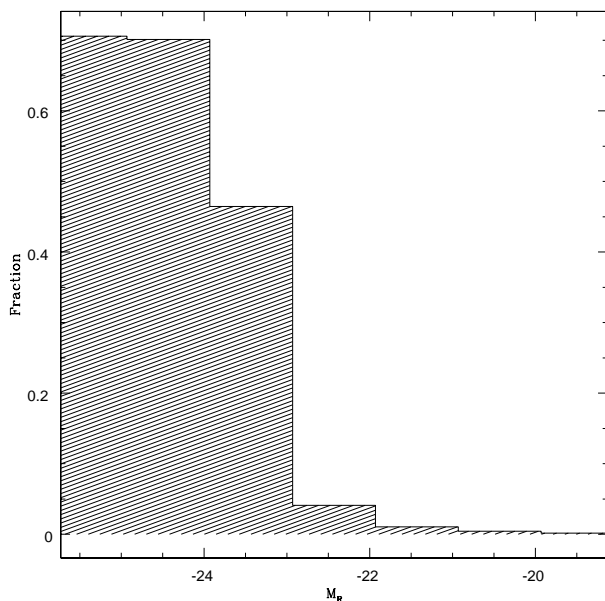
There are too few galaxies in the local Universe ($D < 40$ Mpc; *Nearby Galaxies Catalog*, Tully 1988) for this region of the LF to be measured directly: only one galaxy (the Seyfert galaxy NGC 4594) has $M_R < -24$ and 25 have $M_R < -23$. For $D < 40$ Mpc, the ratio of galaxies with $-24 < M_R < -23.5$ to those with $-23.5 < M_R < -23$ is 0.20 ± 0.11 . The LF shown in Figure 1 implies a value for this ratio of 0.09, consistent with the number for the local Universe number. This concordance suggests that the evolutionary corrections made to the SDSS data, which are computed using observations of galaxies whose absolute magnitudes span a wide range, are appropriate at the very bright end $M_R < -23$.

4 RESULTS FROM DEEP MOSAIC CCD SURVEYS

In Table 2 we list some nearby groups where deep CCD mosaic imaging has been performed. The LFs from these surveys extend down to $M_R = -10$. Earlier photographic studies (e. g. Ferguson & Sandage 1991) covered larger areas but did not reach magnitudes this faint. All of these groups

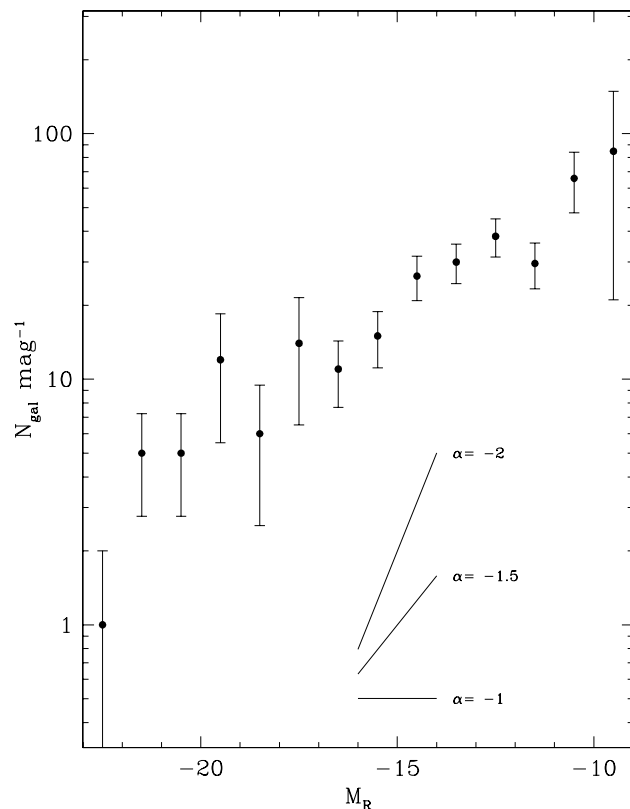
Table 1. Spectroscopic field surveys

Survey	Reference	Filter	Limiting Magnitude
Stromolo-APM	Loveday et al. 1992	b_J	-17
Hawaii-Caltech	Cowie et al. 1996	B	-12.5
		K	-20.5
Autofib	Ellis et al. 1996	b_J	-15
LCRS	Lin et al. 1996	R	-18
ESO Slice Project	Zucca et al. 1997	b_J	-15
SDSS	Blanton et al. 2001, 2003	u'	-16.5
		g'	-17.5
		r'	-17
		i'	-18
		z'	-19.5
2MASS +2df	Cole et al. 2001	J	-19
		K_s	-20
2df	Norberg et al. 2002	b_J	-17.5


Figure 2. The fraction of galaxies at redshift $z > 0.2$ in the SDSS sample used to compile Figure 1.

have been imaged in the Cousins R band ($\lambda_{\text{eff}} = 6588 \text{ \AA}$), which is close to the SDSS r' band ($\lambda_{\text{eff}} = 6290 \text{ \AA}$; Fukugita et al. 1995). The R -band LF of these groups is therefore suitable for extending the SDSS LF to faint magnitudes.

Members are identified based on their surface brightnesses. Low-surface-brightness galaxies that appear within a group of giant galaxies and whose counterparts do not exist in blank fields are assumed to lie at the distance of the group. Distances are therefore determined based on morphology; spectroscopic redshifts are unattainable for these faint low-surface-brightness galaxies. At the faintest magnitudes this exercise becomes statistical as a few very small low-surface-brightness galaxies are visible in blank fields. We tend to see more such galaxies in fields containing nearby


Figure 3. The composite luminosity function for the groups listed in Table 2, with errors computed as described in the text. Here N_{gal} is the total number of galaxies in the combined sample, proportional to N in Figure 1.

groups of large galaxies, but for any particular galaxy we can only assign membership on probabilistic grounds.

The composite LF of the groups in Table 2 is presented in Figure 3. Computing this was not straightforward because of the different methods used by different authors to

Table 2. Groups with deep luminosity function measurements

Group	Distance Mpc	limiting M_R	reference	survey telescope	sample size
Ursa Major	18.6	-11	Trentham et al. 2001a (TTV01)	CFHT	50
Leo I	11.1	-10	Flint et al. 2001b	KPNO 0.9 m	112
Coma I	16.4	-10	Trentham & Tully 2002 (TT02)	Subaru	38
NGC 1023 Group	10.0	-10	Trentham & Tully 2002 (TT02)	Subaru	28

assess membership probabilities. For Ursa Major, Coma I, and the NGC 1023 Group (hereafter G1), TTV01 and TT02 employed a subjective rating system based on surface brightnesses, morphologies and spectroscopy (when available). For the present calculation, galaxies were assigned a high (rating “0–2” in the notation of TTV01 and TT02) or low (rating “3”) probability of membership. For the Leo I Group (hereafter G2), Flint, Bolte & Mendes de Olivera (2001b) computed completeness corrections $C(M)$ in each magnitude interval. The number of galaxies in the composite group sample in each magnitude interval equals the number of G1 galaxies with a high membership probability plus 1/2 times the the number of G1 galaxies with a low membership probability plus $(1 + C(M))$ times the number of galaxies in the G2 sample. The weighting of 1/2 for the G1 galaxies with a low membership probability comes from a study of the radial distribution of galaxies with this rating within the groups (TTV01, TT02).

The uncertainties in these numbers are potentially large because the rating system used by TTV01 and TT02 is subjective and the completeness corrections used for the G2 sample are model-dependant. Errors in the number of group members will be systematic and a conservative approach will be required to determine the uncertainties; we estimate them from the quadrature sum of Poisson errors (Gehrels 1986), the entire contribution of G1 galaxies with a low membership probability and the entire enhancement in the number of G2 galaxies due to completeness corrections. That the error bars in Figure 3 are so large at the faintest magnitudes follows from the fact that the contributions from the last two terms dominate the uncertainties.

The LF of the groups over the range $M_R = -19$ to $M_R = -10$ is fit by a power law of index $\alpha = -1.26 \pm 0.11$. This is an interesting magnitude range because $M_R = -19$ ($M_B \sim -18$) is the brightest magnitude where dwarf galaxies, as identified by their position on a magnitude–surface-brightness plot (e. g. Figure 1 of Binggeli 1994), contribute significantly to the LF.

Precise distances have been measured to individual low-luminosity galaxies in Centaurus and Sculptor (Jerjen, Freeman & Binggeli 2000; Karachentsev et al. 2002). These groups will be good candidates to add to the list in Table 2 when complete galaxy samples are available; this will reduce the errors in Figure 3.

5 THE LOCAL GROUP

The LF of groups has large errors at $M_R \sim -10$ which can be decreased by including the Local Group in the analysis. In the Local Group, the lowest-luminosity galaxies can be resolved into stars so that membership can be established with confidence. However, there are very few galaxies and the Poisson errors are large (but not significantly larger than the errors in the LF of groups at $M_R \sim -10$).

The faintest galaxies in the Local Group would have been detected in the nearby groups studied by Trentham & Tully 2002 given the detection limit of that survey (1σ of about 29 R mag arcsec $^{-2}$). However only a small part of the galaxies would be visible above the sky and the galaxies would be indistinguishable from a large number of small background galaxies, many of which have been dimmed by $(1+z)^4$ cosmological effects. The ability to distinguish members from background galaxies can only be performed with any confidence brighter than $M_R = -10$.

There are, however, complications in deriving a Local Group LF that can used in the current analysis.

Firstly there are uncertainties as to the membership of stars in specific galaxies. For example, in Draco, inclusion of a number of new stars caused the tidal radius to increase significantly (Piatek et al. 2001 Odenkirchen et al. 2001) which in turn caused the absolute magnitude to brighten. Therefore absolute magnitudes of individual Local Group galaxies are uncertain.

Secondly, most Local Group galaxies have not been observed in the R -band. Therefore we need to perform a colour correction for each dwarf.

Thirdly, the Local Group sample may be incomplete at the faint end. The lowest-luminosity galaxies have very low surface brightnesses and so can be difficult to find. They are particularly difficult to find if they are viewed in projection against either the Milky Way or the M31 disks (e. g. Andromeda IX; Zucker et al. 2004). They are also difficult to find if they are in the process of being disrupted (e. g. Sagittarius; Ibata, Gilmore & Irwin 1994, 1995).

Furthermore, it can be possible to identify groups of stars but be uncertain as to whether or not these stars form part of a discrete galaxy with a dark halo. Including or excluding such objects from the Local Group galaxy sample can then be subjective. An example is Andromeda VIII (Morrison et al. 2003), which may be part of the M31 stream (Ibata et al. 2004). Another example is Canis Major (Martin et al. 2004, Momany et al. 2004).

In Table 3 we present a list of Local Group members and their absolute R -band magnitudes. The methods used to de-

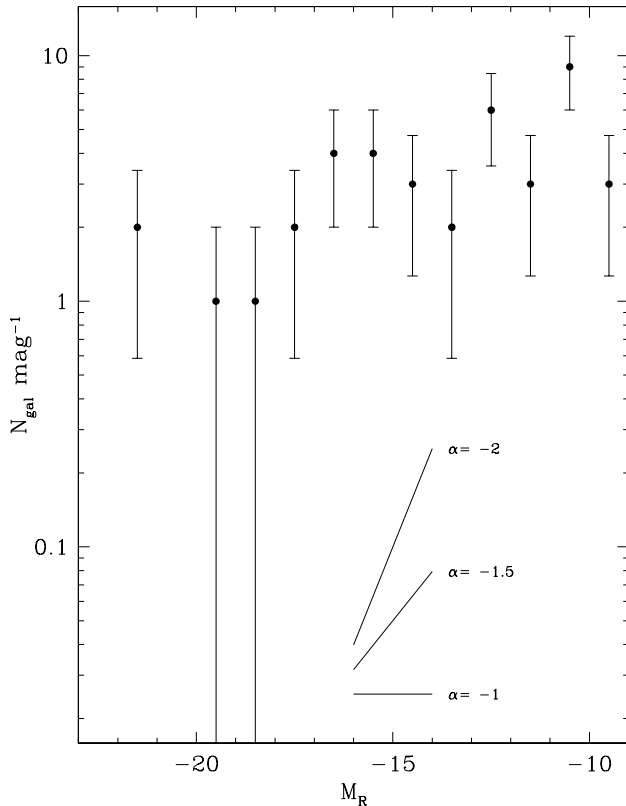


Figure 4. The luminosity function of the Local Group.

rive these magnitudes are: [1] interpolation using the spectral energy distributions (SEDs) of Fukugita et al. (1995; hereafter F95), adopting a literature value for the absolute magnitude in some filter, and choosing a SED appropriate for the Hubble type of the galaxy; [2] as [1] but choosing a SED appropriate for a galaxy with broadband colours equal to those measured for the galaxy; [3] as [1] but choosing a SED appropriate for a galaxy with broadband colours equal to those inferred from colour-magnitude diagrams; [4] adopting a literature value for M_R .

The LF for the Local Group is presented in Figure 4. The faint-end slope is $\alpha = -1.1 \pm 0.1$, consistent with the findings of Pritchett & van den Bergh (1999) and van den Bergh (2000).

Recently Karachentsev et al. (2004) compiled a list of galaxies in the local Universe with distances less than 10 Mpc, the Local Volume (LV) catalogue. This sample is probably incomplete at the very faint end at present but over the next few years it should be possible to identify and measure magnitudes and distances (by, for example, the tip of the red giant branch method) for the vast majority of galaxies within 10 Mpc. This will allow us to generate a LF with much smaller errors than in Figure 4.

6 COMBINING THE MEASUREMENTS – THE GALAXY LF

The field luminosity function, obtained by combining the LFs described in the previous three sections, is presented in

Table 3. Local Group members

Galaxy	type	M_R	method	reference
M31 = NGC 224	Sb	-21.8	1	1
Milky Way	Sbc	-21.5	1	2
M33 = NGC 598	Sc	-19.5	3	2,3
LMC	dI	-18.8	3	2,4
SMC	dI	-17.4	3	2,5
M32 = NGC 221	E	-17.1	2	6,7
NGC 205	dE	-16.9	2	6,7
NGC 6822	dI	-16.5	2	6,7
IC 10	dI	-16.3	2	2,8
NGC 3109	dI	-16.1	2	6,7
NGC 185	dE	-15.7	2	6,7
IC 1613	dI	-15.8	3	6,9
NGC 147	dE	-15.7	2	6,7
Sagittarius	dE	-15.4	3	6,10
Sextans A	dI	-14.9	3	6,11
WLM	dI	-14.7	3	6,12
Sextans B	dI	-14.7	3	6,13
Fornax	dE	-13.6	3	6,14
Pegasus = DDO 216	dI	-13.4	3	6,15
And VII = Cassiopeia	dE	-12.7	3	6,16
Leo I	dE	-12.6	3	6,17
And I	dE	-12.5	3	6,18
And II	dE	-12.5	3	6,18
SagDIG	dE	-12.3	4	19
Leo A	dI	-12.1	3	6,20
Antlia	dE	-11.9	3	6,21
Aquarius = DDO 210	dE	-11.5	3	6,22
And VI = Pegasus	dE	-11.1	3	6,23
LGS 3	dI	-10.9	3	24,25
And III	dE	-10.8	3	18,26
Cetus	dE	-10.7	3	6,27
Leo II	dE	-10.6	3	6,28
Sculptor	dE	-10.3	3	6,29
Phoenix	dE/I	-10.3	3	6,30
Tucana	dE	-10.2	3	6,31
Sextans	dE	-10.1	3	26,32
Draco	dE	-10.0	3	6,33
And V	dE	-9.8	3	34,35
Carina	dE	-9.9	3	1,11,15
Ursa Minor	dE	-9.8	3	34,35
And IX	dE	-8.8	3	1,10

1. SED from NASA/IPAC Extragalactic Database (ned-www.ipac.caltech.edu); 2. van den Bergh 2000; 3. McConnachie et al. 2004; 4. Castro et al. 2001; 5. Alciano et al. 2003; 6. Grebel et al. 2003; 7. Prugniel & Heraudeau 1998; 8. de Vaucouleurs & Ables 1965; 9. Tikhonov & Galazutdinova 2002; 10. Ibata et al. 1997; 11. Dolphin et al. 2003; 12. Rejkuba et al. 2000; 13. Sakai et al. 1997; 14. Bersier & Wood 2002; 15. Gallagher et al. 1998; 16. Grebel & Guhatakurta 1999; 17. Held et al. 2001; 18. Da Costa, Armandroff & Caldwell 2002; 19. Lee & Kim 2000; 20. Dolphin et al. 2002; 21. Tolstoy & Irwin 2000; 22. Lee et al. 1999; 23. Hopp et al. 1999; 24. Lee 1995a; 25. Miller et al. 2001; 26. Caldwell et al. 1992; 27. Sarajedini et al. 2001; 28. Lee 1995b; 29. Monkiewicz et al. 1999; 30. Gallart et al. 2001; 31. Castellani, Marconi & Buonanno 2002; 32. Bellazzini et al. 2001; 33. Klessen, Grebel & Harbeck 2003; 34. Caldwell 1999; 35. Davidge et al. 2002; 36. Rizzi et al. 2003; 37. Zucker et al. 2004

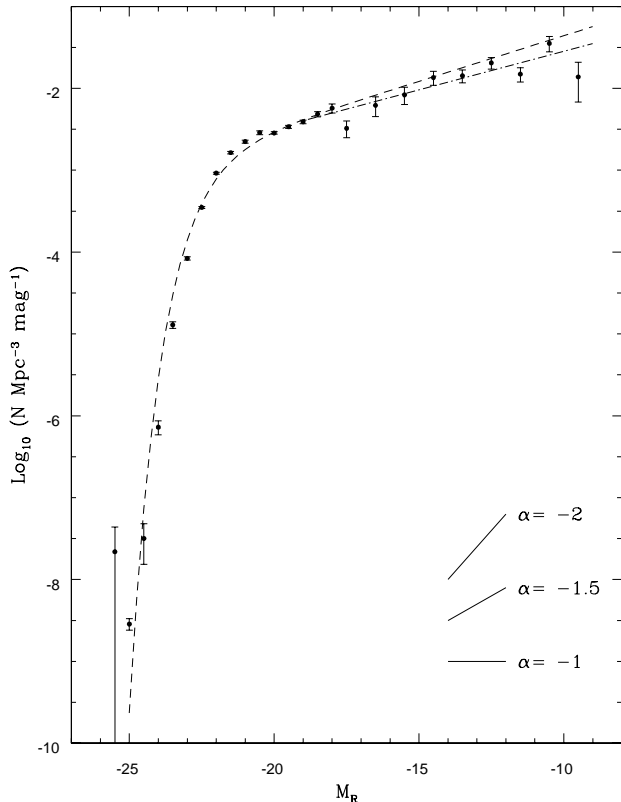


Figure 5. The field galaxy luminosity function. The normalization is as appropriate to the SDSS data and the other samples are grafted onto the SDSS LF. The dashed line shows the best Schechter function fit to all the data: $M_R^* = -22.0$, $\alpha^* = -1.29$. The dotted-dashed line shows the best power-law fit for $M_R > -19$: $\alpha = -1.26$.

Figure 5 and Table 4. Prior to being combined, the LFs were normalized to a consistent scale and were weighted at each magnitude by the inverse of the square of the uncertainty.

Figure 6 shows how much each individual LF contributes to the total LF. The SDSS dominates the LF at the bright end and the CCD mosaic surveys at the faint end. The Local Group is important only for the faintest ($M_R = -9.5$) point.

Two points on the LF are worthy of further discussion: (1) the $M_R = -17.5$ point. This is the faintest point where the SDSS dominates and it is significantly lower than all other points in this region. One possibility is that the SDSS sample is incomplete here because galaxies with this absolute magnitude have surface brightnesses too low for spectroscopy. On the other hand, the majority of galaxies with $M_R = -17.5$ ($M_B \sim -16.5$) have surface brightnesses within their half-light-radius of $\mu_{50} \sim 20 R \text{ mag arcsec}^{-2}$ (Trentham, Tully & Verheijen 2001b), which is bright enough for spectroscopy with the instruments used by SDSS. Another possibility is that galaxies are rare at precisely this magnitude, which corresponds roughly to the transition magnitude between giant and dwarf galaxies. Interestingly, Flint, Bolte & Mendes de Olivera (2003) report a deficiency in galaxies with absolute magnitudes close to this value in the Leo I Group.

Table 4. The Field Galaxy Luminosity Function

M_R	ϕ N mag ⁻¹ Mpc ⁻³
-25.5	$(2.18 \pm 2.18) \times 10^{-8}$
-25.0	$(2.86 \pm 0.46) \times 10^{-9}$
-24.5	$(3.17 \pm 1.64) \times 10^{-8}$
-24.0	$(7.26 \pm 1.40) \times 10^{-7}$
-23.5	$(1.30 \pm 0.12) \times 10^{-5}$
-23.0	$(8.38 \pm 0.36) \times 10^{-5}$
-22.5	$(3.50 \pm 0.091) \times 10^{-4}$
-22.0	0.000920 ± 0.000026
-21.5	0.00164 ± 0.000052
-21.0	0.00224 ± 0.000092
-20.5	0.00288 ± 0.00015
-20.0	0.00285 ± 0.000096
-19.5	0.00339 ± 0.00014
-19.0	0.00390 ± 0.00019
-18.5	0.00483 ± 0.00035
-18.0	0.00573 ± 0.00072
-17.5	0.00325 ± 0.00075
-16.5	0.00694 ± 0.0019
-15.5	0.00931 ± 0.0022
-14.5	0.0150 ± 0.0029
-13.5	0.0156 ± 0.0028
-12.5	0.0228 ± 0.0037
-11.5	0.0166 ± 0.0033
-10.5	0.0393 ± 0.0083
-9.5	0.0151 ± 0.0073

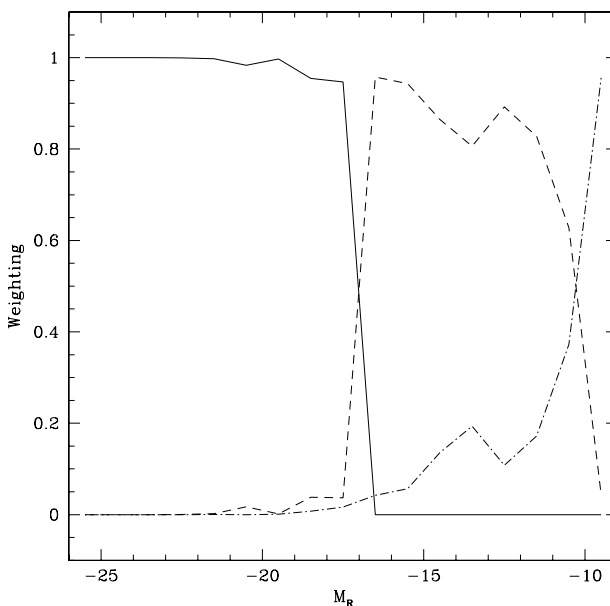


Figure 6. The weighting of each component to the total LF for the SDSS (solid line), CCD mosaic (dashed line) and Local Group (dotted-dashed line) samples. The weightings here are proportional to σ^2 , where σ is the error in the component LF.

(2) the $M_R = -9.5$ point. There are only three Local Group galaxies which contribute to this point, and all narrowly escaped inclusion into the $M_R = -10.5$ bin. While completeness and small number statistics are surely concerns at this extreme faint end, this observation may be a hint of a turnover in the LF at about $M_R = -9.5$. Galaxies like Andromeda IX would then be extremely rare. The shape of the LF here and the possible existence of a turnover should become well-established over the next few years as the LV sample is extended to larger distances and completeness issues in that sample become better understood.

The normalization of the LF is affected by cosmic variance and will vary from survey to survey. The value adopted in Figure 5 comes from SDSS observations which cover 0.3 % of the sky and so should provide a reasonable representation of the cosmological average.

7 ANALYTIC FORMS

A power-law fit to the LF over the range $M_R > -19$ gives a logarithmic slope $\alpha = -1.2$ but this is not a good fit in that it overpredicts the number of galaxies at the extreme faint end. The error bars in Figure 5 are small enough that curvature in the LF within this magnitude range is detectable at a high level of significance.

It is common to fit LFs with Schechter (1976) functions:

$$\phi(L) = \phi^* \exp\left(-\frac{L}{L^*}\right) \left(\frac{L}{L^*}\right)^\alpha \frac{1}{L^*}, \quad (1)$$

or in magnitude units

$$\phi(M) = 0.92 \phi^* (10^{[-0.4(M-M^*)]})^{\alpha^*+1} e^{-10^{[-0.4(M-M^*)]}}. \quad (2)$$

Here ϕ^* is a normalization density, L^* and $M^* = -2.5 \log_{10} L^*$ are a characteristic luminosity and magnitude, and α^* is a characteristic faint-end slope. These fits normally have $\alpha > -2$ and so provide convenient ways to describe galaxy luminosities over a magnitude range (close to M^*) where most of the total luminosity of a sample of galaxies is obtained. Schechter function fits have no physical basis but are attractive in that their exponential cutoff is similar to that predicted by simple analytical models of galaxy formation (e. g. White & Rees 1978).

A Schechter function fit over the entire range $-25 < M_R < -9$ is poor because (1) it is not possible to simultaneously fit the data at both $M_R = -22$ and $M_R = -20$ where the errors in the SDSS LF are so small, (2) the point at $M_R = -17.5$ is systematically too low, and (3) a Schechter function which fits the data well at bright magnitudes then overpredicts the number of faint galaxies. These features are illustrated by the dashed line on Figure 5.

Two-parameter fits cannot fit the data over any significant magnitude range. Composite forms, like linear combinations of Gaussian and Schechter functions, may provide acceptable fits to the data but there is no physical basis for selecting a particular set of functions at this stage.

8 COMPARISON WITH THEORY

It is well known that cold dark matter (CDM) theory predicts a mass function of dark halos that is steep at the low-

mass end (e. g. Moore et al. 1999). Simulations predict a logarithmic mass function slope $\alpha \sim -2$ at low masses.

The field galaxy LF is much shallower than this at all magnitudes. This tells us that star formation must be less efficient in lower-mass galaxies. There are various physical processes that can be responsible for this. Lower-mass galaxies are more susceptible to gas ejection by supernova-driven winds (Dekel & Silk 1986) due to their having smaller gravitational potential wells. This means that negative feedback effects during star formation (Efstathiou 2000) are stronger in lower-mass galaxies. Additionally, in hierarchical clustering cosmologies like CDM, many low-mass galaxies form at later times so it will be difficult for them to collect gas from an intergalactic medium that is being progressively heated by the metagalactic ultraviolet background (Thouly & Weinberg 1996; Klypin et al. 1999; Bullock, Kravtsov & Weinberg 2001; Tully et al. 2002).

Whatever processes are responsible, we shall see below that they must operate less efficiently in galaxy clusters. Perhaps the presence of a confining medium (Babul & Rees 1992) inhibits the effects of negative feedback during low-mass galaxy formation (see Section 5 of Roberts et al. 2004).

9 THE CLUSTER LF

Various measurements of cluster LFs have been made possible by a number of advances in technology.

The prototypical rich galaxy cluster is the Coma cluster, with several hundred galaxies brighter than $M_R = -19$ per square degree. Recently a spectroscopic LF of Coma extending down to $M_R = -16$ has been published (Mobasher et al. 2003). This is a difficult measurement to make because it requires spectroscopy of large numbers of faint sources, many of which have relatively low surface brightnesses. This measurement has been made possible by the advent of wide-field multi-object spectrographs that can be used on large telescopes, in this case WYFFOS on the 4.2 m William Herschel Telescope (Bridges 1998).

Many other clusters that are richer and more distant than Coma have also been studied (A665 at $z = 0.18$: the only Abell (1958) Richness 5 cluster, Wilson et al. 1997, Trentham 1998; A963 at $z = 0.21$, Driver et al. 1994, Trentham 1998; A1689 at $z = 0.18$, Wilson et al. 1997; A868 at $z = 0.15$, Boyce et al. 2001; A1146 at $z = 0.14$, Trentham 1997). These clusters have very well-determined LFs at the bright end because their contrast against the background field galaxy population is so high. Photometry alone can therefore be used for a measurement of the LF at bright absolute magnitudes. When many such clusters are considered in conjunction with each other, the numbers of galaxies in each bin becomes large and the Poisson errors are consequently small. At the faint end, these measurements cannot be used to determine the LF since the cluster counts are small compared to the background counts and the field-to-field variance of the background is much larger than the cluster signal. Spectroscopic measurements cannot help either at the faint end since the clusters are so distant.

The Virgo cluster is much less rich than the Coma Cluster, but at 17 Mpc it is sufficiently nearby that dwarf galaxies are much larger than the seeing and can be identified by their low surface brightnesses. The LF can then be determined

to faint limits by photometric observations alone. This LF will not include the contribution from compact galaxies like M32 and the Ultra Compact Dwarfs in the Fornax Cluster (Phillipps et al. 2001, Drinkwater et al. 2003) because they will be mis-identified as background ellipticals. However these types of galaxies are rare. The Virgo Cluster Catalog (Binggeli, Sandage & Tammann 1985) was compiled about 20 years ago and provided a precise measurement of the bright end of Virgo Cluster LF (Sandage, Binggeli & Tammann 1985). More recently, mosaic CCD measurements (Trentham & Hodgkin 2002, Sabatini et al. 2003) using the Wide Field Camera on the 2.5 m Isaac Newton Telescope (INT) have confirmed the earlier results and have extended the LF faintward by about 5 magnitudes. Extremely deep observations over a smaller area of Virgo using SuprimeCam on the 8 m Subaru Telescope (Trentham & Tully 2002) did not result in the discovery of any new dwarfs brighter than the completeness limit of the INT survey (about $M_B = -11$) that were too low in surface brightnesses to be seen with the smaller telescope. The implication is then that the LF of the Virgo Cluster is known at least as faint as $M_B = -11$.

We derive a composite cluster LF by combining measurements from photometric studies of rich galaxy clusters (A665, A963, A1795, A2199 and A1146; Trentham 1997, 1998), the deep spectroscopic study of the Coma cluster (Mobasher et al. 2003), and a photometric study of the Virgo cluster (Trentham & Hodgkin 2002). Each dataset is important in a different absolute magnitude regime (Figure 7). At very bright absolute magnitudes, the rich cluster sample is most important; the Coma and Virgo samples suffer from small number statistics. At intermediate magnitudes, the Coma sample is most important; the rich cluster LF has large errors since a background subtraction is required and the background has a large field-to-field variance and the Virgo sample has substantial Poisson errors. At faint magnitudes only the Virgo data can be used; the other surveys cannot detect dwarfs, most of which have low surface brightnesses. Although the three samples utilise very different methods in establishing membership, they are consistent with each other in the absolute magnitude where they overlap. All data used are R -band data except the Virgo data which are B -band data converted to the R -band using a combination of (1) $B - R$ colours from a calibration derived using measurements of faint galaxies observed in both the INT and Subaru surveys, (2) the spectral energy distributions from F95, and (3) the $B - R$ calibration for giant galaxies of different Hubble Type T obtained using data from Tully & Pierce (2000): $B - R = 1.40 - 0.059T$ (equation (1) in TT02). Typical random errors in this conversion are estimated to be 0.1 – 0.2 mag, smaller than the bin size of 0.5 mag.

The cluster LF is presented in Table 5 and Figure 8. This LF is appropriate for centres of galaxy clusters although the inclusion or exclusion of cD galaxies in the samples used to define the LF is arbitrary. There is evidence, however, that the LF might be quite different in the outer parts of galaxy clusters (Phillipps et al. 1998).

The cluster LF can be fit by a Schechter function brightward of $M_R = -16$, where it rises with a logarithmic slope $\alpha = -1.6$ and then is flat faintward of about $M_R = -13$. The faintest point on the LF shown in Figure 8 might be affected by incompleteness (although the deep Subaru Virgo

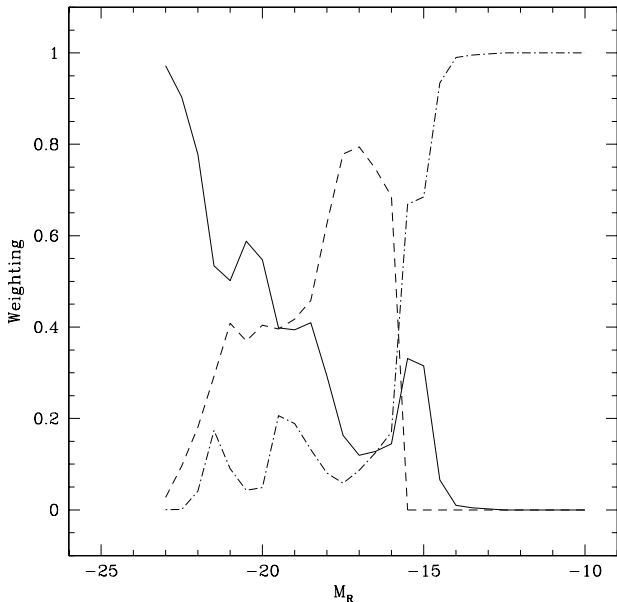


Figure 7. The weighting of each component to the total LF. The lines are for the rich cluster (solid line), Coma (dashed line) and Virgo (dotted-dashed line) samples. The weightings here are proportional to σ^{-2} , where σ is the error in the component LF.

Table 5. The Galaxy Cluster Luminosity Function

M_R	ϕ N mag $^{-1}$ Mpc $^{-3}$
-23.0	0.88 ± 0.61
-22.5	1.46 ± 0.80
-22.0	16.2 ± 4.0
-21.5	33.4 ± 5.8
-21.0	57.3 ± 7.2
-20.5	78.5 ± 8.6
-20.0	84.2 ± 9.2
-19.5	72.9 ± 8.9
-19.0	89.1 ± 10.4
-18.5	113 ± 12
-18.0	101 ± 13
-17.5	152 ± 11
-17.0	150 ± 14
-16.5	214 ± 19
-16.0	180 ± 26
-15.5	366 ± 65
-15.0	404 ± 71
-14.5	599 ± 89
-14.0	551 ± 87
-13.5	577 ± 89
-13.0	561 ± 88
-12.5	558 ± 88
-12.0	460 ± 80
-11.5	250 ± 59

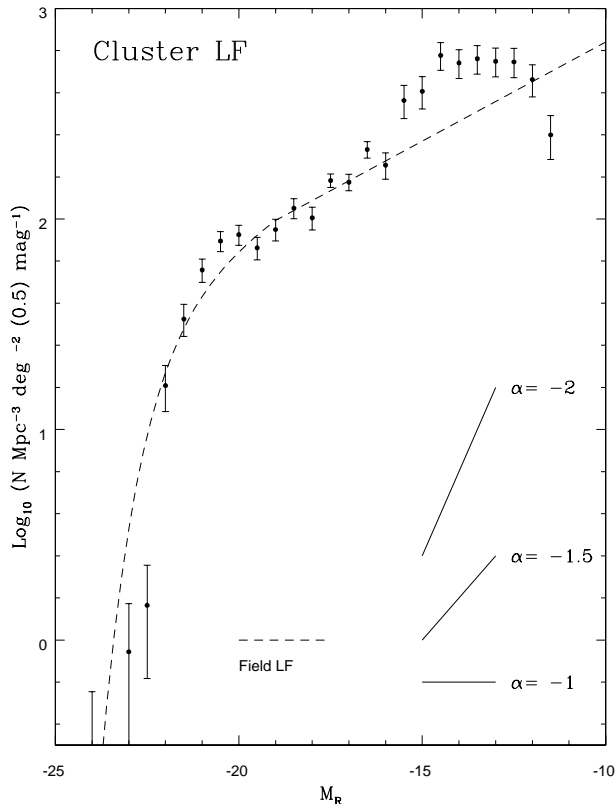


Figure 8. The galaxy cluster luminosity function, computed as described in the text. The normalization is arbitrarily chosen to be that appropriate for the Coma Cluster at $M_R = -21$. The dashed line is the best-fitting field luminosity function, which we approximate by a Schechter function with $M_R^* = -22.0$ and $\alpha^* = -1.28$ brightward of $M_R = -19$ and a power law with $\alpha = -1.24$ faintward of $M_R = -19$.

measurements suggest otherwise) but the flattening faintward of about $M_R = -13$ comes from an analysis of the Virgo data in an absolute magnitude regime where the completeness is close to 100 per cent.

The field and cluster LFs are highly inconsistent with each other (Figure 9). Brighter than $M_R = -20$, the LF falls off slightly more steeply in the field than in clusters due to the presence of luminous elliptical galaxies in clusters. At about $M_R = -20$, the field and cluster LFs have similar shapes, despite being dominated by contributions from different kinds of galaxies (early-type galaxies in clusters and late-type galaxies in the field). The cluster LF becomes significantly steeper than the field LF at about $M_R = -17$ due to the presence of a large number of dwarf elliptical galaxies. Both LFs are reasonably flat faintward of about $M_R = -15$, although the cluster LF has a higher normalization relative to the giant galaxies than does the field LF and the contribution of dwarf irregular galaxies relative to that of dwarf elliptical galaxies is higher in the field than in clusters. This excess number of cluster relative to field dwarfs is described and studied in detail by Roberts et al. (2004), although the differential between the cluster and field that we find is less than that found by those authors. This may be due in part due to there being slightly fewer dwarfs per giant in groups

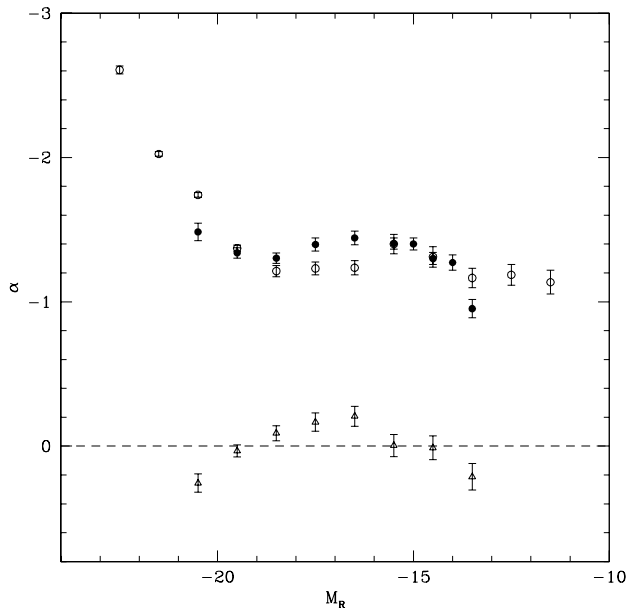


Figure 9. The logarithmic slope α of the field (open circles) and cluster (filled circles) LFs, and the difference between the two (open triangles). The points are calculated at each absolute magnitude M_R by considering the shape of the LF over a two magnitude interval centred on M_R .

than in environments with very low galaxy densities (see Zabludoff & Mulchaey 2000).

The faint end of the cluster luminosity function depends on measurements of the Virgo Cluster and it is important to establish that this environment is representative – different studies of the faint end of the Virgo LF (Trentham & Hodgkin 2002, Trentham & Tully 2002, Sabatini et al. 2003) concur as regards the general shape (rise at $M_R = -17$ and flattening at fainter magnitudes) but comparisons between different clusters at the very faint end have yet to be made. There is a hint of a LF with a similar shape in the knot of early-type galaxies around NGC 1407 (Trentham & Tully 2002) but this sample is small. The best place to determine a LF that can be compared with the Virgo LF is the Fornax Cluster, which also has a population of low-surface-brightness dwarf galaxies (Kambas et al. 2000). Spectroscopic information is available for a subset (about one-quarter) of the Fornax Cluster Spectroscopic Survey (FCSS) dwarfs, but there are too few dwarfs known (19 with $-15.8 < M_B < -12.7$; Deady et al. 2002) for a LF to be computed that can be compared in detail with the Virgo LF. When the FCSS is complete, this will be an important comparison.

The previous paragraph is concerned with the precise shape of the LF at the faintest magnitudes. All current evidence does at this stage points towards an excess of low-luminosity galaxies in clusters, although this precise shape depends on the measurements of the local clusters. For example, an excess of low luminosity cluster galaxies above the expected number given the field LF was seen in the 2dF redshift survey (de Propris et al. 2003).

This tendency for dwarfs to be more numerous in the richer and denser environments is important in that it tells

us that the physical processes responsible for suppressing the formation of stars in low-mass dwarf galaxies may operate less efficiently in clusters than in the field. Alternatively there are additional physical processes that operate preferentially in clusters and alleviate the effects of dwarf suppression there. For a more detailed discussion of these issues, the reader is referred to Roberts et al. (2004).

The shape of the cluster LF is such that it cannot be described by a simple analytic form. Composite forms may be more appropriate; these may provide a useful test of theories which may wish to invoke different formation mechanisms for giant and dwarf galaxies. For example, the cluster LF is well fit by a double Schechter function with $(M^*, \alpha^*) = (-21.4, -1.0)$ for giants and $(M^*, \alpha^*) = (-16.6, -1.1)$ for dwarfs and a relative normalization of $2.7 \times 10^{-0.4(M_{\text{giant}}^* - M_{\text{dwarf}}^*)}$.

10 SUMMARY

This paper presents the results of a study that combines different datasets in order to measure the field galaxy LF over the range $-25 < M_R < -9$. The data come from the Sloan Digital Sky Survey, from CCD mosaic imaging surveys of nearby groups, and from the Local Group. The field luminosity function is well-described by a Schechter function with $M_R^* = -22.0$ and $\alpha^* = -1.28$ brightward of $M_R = -19$ and by a power law with $\alpha = -1.24$ faintward of $M_R = -19$. This is shallower than the CDM mass function ($\alpha \sim -2$), implying that star formation is less efficient in lower-mass galaxies.

A similar analysis was performed to measure the LF of galaxy clusters. The three samples used were a photometric survey of rich Abell clusters, a spectroscopic survey of the Coma Cluster and a photometric survey of the Virgo Cluster. The cluster LF differs from the field LF in that it has a rise of $\alpha \sim -1.6$ between $M_R = -17$ and $M_R = -14$, although it flattens faintward of $M_R = -14$. In the context of CDM theories, this suggests that the physical processes that are responsible for suppressing the formation of stars in low-mass galaxies operate less efficiently in clusters than in the field.

ACKNOWLEDGEMENTS

This research has made use of the NASA/IPAC Extragalactic Database (NED) which is operated by the Jet Propulsion Laboratory, Caltech, under agreement with the National Aeronautics and Space Association.

REFERENCES

Abell G. O., 1958, *ApJS*, 3, 211
 Alcaino G., Alvarado F., Borissova J., Kurtev R., *A&A*, 2003, 400, 917
 Babul A., Rees M. J., 1992, 255, 346
 Bellazzini M., Ferraro F. R., Pancino E., 2001, *MNRAS*, 327, L15
 Benson A. J., Bower R. G., Frenk C. S., Lacey C. G., Baugh C. M., Cole S., 2003a, *ApJ*, 599, 38
 Benson A. J., Frenk C. S., Baugh C. M., Cole S., Lacey C. G., 2003b, *MNRAS*, 343, 679

Bersier D., Wood P. R., 2002, *AJ*, 123, 840
 Binggeli B., 1994, in Meylan G., Prugneil P., ed., *ESO Conference and Workshop Proceedings No. 49: Dwarf Galaxies*. European Space Observatory, Munich, p. 13
 Binggeli B., Sandage A., Tammann G. A., 1985, *AJ*, 90, 1681
 Blanton M. R. et al., 2001, *AJ*, 121, 2358
 Blanton M. R. et al., 2003, *ApJ*, 592, 819
 Boyce P. J., Phillipps S., Jones J. B., Driver S. P., Smith R. M., Couch W. J., 2001, *MNRAS*, 328, 277
 Bridges T., 1998, in Arribas S., Mediavilla E., Watson F., eds., *Fiber Optics in Astronomy III*, ASP Conference Series Vol. 152, p. 104
 Bullock J. S., Kravstov A. V., Weinberg D. H., 2001, *ApJ*, 548, 33
 Caldwell N., 1999, *AJ*, 118, 1230
 Caldwell N., Armandroff T. E., Seitzer P., Da Costa G. S., 1992, *AJ*, 108, 840
 Castellani M., Marconi G., Buonanno R., 1996, *A&A*, 310, 715
 Castro R., Santiago B. X., Gilmore G. F., Beaulieu S., Johnson R. A., 2001, *MNRAS*, 326, 333
 Chiu W. A., Gnedin N. Y., Ostriker J. P., 2001, *ApJ*, 563, 21
 Cole S. et al., 2001, *MNRAS*, 326, 255
 Cowie L. L., Songaila A., Hu E. M., Cohen J. G., 1996, *AJ*, 112, 839
 Cross N. et al., 2001, *MNRAS*, 324, 825
 Da Costa G. S., Armandroff T. E., Caldwell N., 2002, *AJ*, 124, 332
 Davidge T. J., Da Costa G. S., Jorgensen I., Allington-Smith J. R., 2002, *AJ*, 124, 886
 Deady J. H., Boyce P. J., Phillipps S., Drinkwater M. J., Karick A., Jones J. B., Gregg M. D., Smith R. M., 2002, *MNRAS*, 336, 851
 Dekel A., Silk J., 1986, *ApJ*, 303, 39
 de Propris R. et al., 2003, *MNRAS*, 342, 725
 de Vaucouleurs G., Ables H., 1965, 77, 277
 Dolphin A. E. et al., 2002, *AJ*, 123, 3154
 Dolphin A. E. et al., 2003, *AJ*, 126, 187
 Drinkwater M. J., Gregg M. D., Hilker M., Bekki K., Couch W. J., Ferguson H. C., Jones J. B., Phillipps S., 2003, *Nat*, 423, 519
 Driver S. P., Phillipps S., Davies J. I., Morgan I., Disney M. J., 1994, *MNRAS*, 266, 155
 Efsthathiou G., 2000, *MNRAS*, 317, 697
 Ellis R. S., Colless M., Broadhurst T., Heyl J., Glazebrook K., 1996, *MNRAS*, 280, 235
 Ferguson H. C., Sandage A., 1991, *AJ*, 101, 765
 Flint K., Metevier A. J., Bolte M., Mendes de Oliveira C., 2001a, *ApJS*, 134, 53
 Flint K., Bolte M., Mendes de Oliveira C., 2001b, in de Boer K. S., Dettmar R.-J., Klein U., eds, *Dwarf Galaxies and their environment*. Shaker Verlag, Aachen, p. 209
 Flint K., Bolte M., Mendes de Oliveira C., 2003, *Ap&SS*, 285, 191
 Fukugita M., Shimasaku K., Ichikawa T., 1995, *PASP*, 107, 945
 Gallagher J. S., Tolstoy E., Dohm-Palmer R. C., Skillman E. D., Cole A. A., Hoessel J. G., Saha A., Mateo M., 1998, *AJ*, 115, 1869
 Gallart C., Martinez-Delgado D., Gomez-Flechoso M. A., Mateo M., 2001, *AJ*, 1221, 2572
 Gehrels N., 1986, *ApJ*, 303, 336
 Grebel E. K., Guhathakurta P., 1999, *AJ*, 511, L101
 Grebel E. K., Gallagher J. S. III., Harbeck D., 2003, *AJ*, 125, 1926
 Held E. V., Clementini G., Rizzi L., Momany Y., Saviane I., Di Fabrizio L., 2001, *AJ*, 562, L39
 Hopp U., Schulte-Ladbeck R. E., Greggio L., Mehlert D., 1999, *A&A*, 342, L9
 Iбата R., Chapman S., Ferguson A. M. N., Irwin M., Lewis G., McConnachie A., 2004, *MNRAS*, 351, 117
 Iбата R., Gilmore G., Irwin M. J., 1994, *Nat*, 370, 194

- Ibata R., Gilmore G., Irwin M. J., 1995, MNRAS, 277, 781
 Ibata R., Wyse R. F. G., Gilmore G., Irwin M. J., Suntzeff N. B., 1997, AJ, 113, 634
 Jerjen H., Freeman K. C., Binggeli B., 2000, AJ, 119, 166
 Kambas A., Davies J. I., Smith R. M., Bianchi S., Haynes J. A., 2000, AJ, 120, 1316
 Karachentsev I. D. et al., 2002, A&A, 385, 21
 Karachentsev I. D., Karachentseva V. E., Huchtmeier W. K., Makarov D. I., 2004, AJ, 127, 2031
 Kazantzidis S., Mayer L., Mastropietro C., Diemand J., Stadel J., Moore B., 2004, ApJ, 608, 663
 Klessen R. S., Grebel E. K., Harbeck D., 2003, ApJ, 589, 798
 Klypin A., Kravtsov A., Valenzuela O., Prada F., 1999, ApJ, 522, 82
 Lee M. G., 1995a, AJ, 110, 1129
 Lee M. G., 1995b, AJ, 110, 1155
 Lee M. G., Aparicio A., Tikonov N., Byun Y. I., Kim E., 1999, AJ, 118, 853
 Lee, M. G., Kim, S. C., 2000, AJ, 119, 777
 Lin H., Kirshner R. P., Shectman S. A., Landy S. D., Oemler A., Tucker D. L., Schechter P. L., 1996, ApJ, 464, 60
 Lin H., Yee H. K. C., Calrberg R. G., Morris S. L., Sawicki M., Patton D. R., Wirth G., Shepherd C. W., 1999, ApJ, 518, 533
 Loveday J., Peterson B. A., Efstathiou G., Maddox S. J., 1992, ApJ, 390, 338
 McConnachie A. W., Irwin M. J., Ferguson A. M. N., Ibata R. A., Lewis G. F., Tanvir N., 2004, MNRAS, 350, 243
 Martin N. F., Ibata R. A., Bellazzini M., Irwin M. J., Lewis G. F., Dehnen W., 2004, MNRAS, 348, 12
 Miller B. W., Dolphin A. E., Lee M. G., Kim S. C., Hodge P., 2001, ApJ, 562, 713
 Miyazaki S. et al., 2002, PASJ, 54, 833
 Mobasher B. et al., 2003, ApJ, 587, 605
 Momany Y., Zaggia S. R., Bonifacio P., Piotto G., De Angeli F., Bedin L. R., Carraro G., 2004, A&A, 421, L29
 Monkiewicz J. et al. 1999, PASP, 111, 1392
 Moore B., Ghigna S., Governato F., Lake G., Quinn T., Stadel J., Tozzi P., 1999, ApJ, 524, L19
 Morrison H. L., Harding P., Hurley-Keller D., Jacoby G., 2003, ApJ, 596, L183
 Norberg P. et al., 2002, MNRAS, 336, 907
 Odenkichen M. et al., AJ, 122, 2538
 Phillipps S., Driver S. P., Couch W. J., Smith R. M., 1998, ApJ, 498, L119
 Phillipps S., Drinkwater M. J., Gregg M. D., Jones J. B., 2001, ApJ, 560, 201
 Piatek S., Pryor C., Armandroff T. E., Olszewski E. W., 2001, AJ, 121, 841
 Pritchett C. J., van den Bergh S., 1999, AJ, 118, 883
 Prugniel P., Heraudeau P., 1998, A&AS, 128, 299
 Rejkuba M., Minniti D., Gregg M. D., Zijlstra A. A., Alonso V. M., Goudfrooij P., 2000, AJ, 120, 801
 Rizzi L., Held E. V., Bertelli G., Saviane I., 2003, AJ, 589, L85
 Roberts S., Davies J., Sabatini S., van Driel W., O'Neil K., Baes M., Linder S., Smith R., Evans R., 2004, MNRAS, 352, 478
 Sabatini S., Davies J., Scaramella R., Smith R., Baes M., Linder S., Roberts S., Testa V., 2003, MNRAS, 341, 981
 Sakai S., Madore B. F., Freedman W. L., 1997, ApJ, 480, 589
 Sandage A., Binggeli B., Tammann G. A., 1985, AJ, 90, 1759
 Sarajedini A. et al., 2002, ApJ, 567, 915
 Schechter P., 1976, ApJ, 203, 297
 Thoul A. A., Weinberg D. H., 1996, ApJ, 465, 608
 Tikhonov N. A., Galazutdinova O. A., 2002, A&A, 394, 33
 Tolstoy E., Irwin M., 2000, MNRAS, 318, 1241
 Trentham N., 1997, MNRAS, 290, 334
 Trentham N., 1998, MNRAS, 295, 360
 Trentham N., Tully R. B., Verheijen M. A. W., 2001a, MNRAS, 325, 385
 Trentham N., Tully R. B., Verheijen M. A. W., 2001b, MNRAS, 325, 1275
 Trentham N., Hodgkin S., 2002, MNRAS, 333, 423
 Trentham N., Tully R. B., 2002, MNRAS, 335, 712
 Tully R. B., Pierce M. J., 2000, ApJ, 533, 744
 Tully R. B., 1988, Nearby Galaxies Catalog, Cambridge University Press
 Tully R. B., Somerville R. S., Trentham N., Verheijen M. A. W., 2002, ApJ, 569, 573
 van den Bergh S., 2000, PASP, 112, 529
 White S. D. M., Rees M. J., 1978, MNRAS, 183, 321
 Wilson G., Smail I., Ellis R. S., Couch W. J., 1997, MNRAS, 284, 915
 Zabludoff A. I., Mulchaey J. S., 2000, ApJ, 539, 136
 Zucca E. et al., 1997, A&A, 326, 477
 Zucker D. L. et al., 2004, ApJ, 612, 121